

論文

[2181] Plastic-Fracture Stress Transfer Model for Concrete Discontinuities

Zhishen WU *, Ahmed M. FARAHAT * and Tada-aki TANABE *

1. INTRODUCTION

The use of non-linear mathematical models for the behavior of concrete structure is becoming increasingly popular. The results obtained using these models, however, will be accurate only if realistic material properties and adequate mechanism are incorporated. Also, the models of general use are necessary to be amenable to the implementation in the numerical procedure such as the finite element method. For these reasons, one of the components in the behavior of concrete structures which could not be satisfactory described up to now is the mechanism of shear transfer across the cracks. Although a great number of macroscopic models have been constructed to deal with the shear transfer problem, none of those models can clearly express the detailed distribution of stresses across the crack. Although some theoretical models have been also proposed, none of those models can deal with the problem to consider the detailed mechanism and surface degradation of contact until crushing at the contact zone.

In the present study, a new motivated constitutive law for the behavior of concrete discontinuities with contact surface degradation and material nonlinearity is presented. Both plastic and fracture deformations with the accumulated damage are formulated at the microlevel. By paying attention to the detailed contact mechanisms both for the contact between mortar and mortar and that between aggregate and mortar, the total deformation are assumed to be due to the aggregate interlock and the degradation of mortar surface. The degradation of mortar surface is expressed by the degradation of the original asperity angle due to the current accumulated damage. Moreover, to simulate all sorts of the nonlinearities, Mohr - Coulomb yield surface in stress space is modified. This modification contains the moving of the subsequent yield surface due to the variation of cohesion, internal angle of friction, and tensile strength because of the accumulated damage. The proposed model showed its capability to predict the experimental data.

2. THEORETICAL APPROACH OF THE PROPOSED MODEL

As shown in Fig.1, the cracked concrete is idealized to have plastic-fracture zone around the crack surfaces while the remaining part is assumed to behave as an elastic material. Furthermore, the geometry of the crack surfaces is idealized to consider both the aggregate interlock and the fracture of mortar. To simulate the fracture of mortar, the crack surfaces are assumed to have sawtooth asperities as shown in Fig.2. Moreover, the phenomenon of aggregate interlock is introduced as shown in Fig.2. In the present study, the analysis is focused at the crack interfaces where the plastic and fracture deformations are likely to occur.

* Department of Civil Engineering, Nagoya University

2.1 SURFACE DEGRADATION

The concept of surface degradation is used to distinguish from the geometrical nonlinearities of the contact zone. As shown in Fig.2, the asperity angles α_m and α_a for both mortar-mortar and aggregate-mortar interfaces have been tentatively expressed in terms of damage parameter ω as follows:

$$\alpha_m = F_1(\omega) = \alpha_0 \exp^{-a\omega} \quad (1)$$

$$\alpha_a = F_2(\omega) = \alpha_n + \left(\frac{\pi}{2} - \alpha_n\right)\sqrt{2\omega - \omega^2} \quad (2)$$

where α_m and α_a are the current asperity angles at mortar-mortar and aggregate-mortar interfaces, α_0 is the initial asperity surface angle, ' a ' is the material degradation parameter. Parameter ' a ' reflects how rapidly the asperity surfaces deteriorate. High and low values of the material parameter ' a ' correspond to brittle and very resistant surface asperities. In this study, the values of $\alpha_0 = 4^\circ$ and ' a ' = 1.0 are selected to obtain a reasonable agreement with the test data. α_n is the initial asperity angle of aggregate-mortar interface due to crack opening ($\alpha_n = 2\delta_N/D$). δ_N is the initial crack opening and ' D ' is the maximum aggregate size (refer to Fig.2).

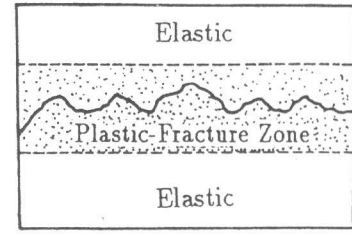


Fig.1 Idealized Concrete

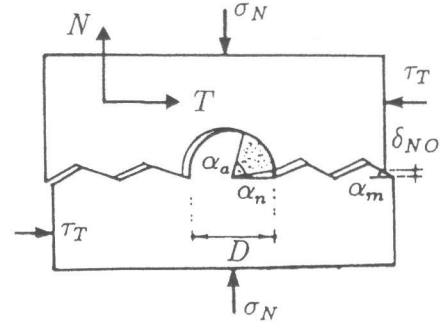


Fig.2 The Notations of Asperity Angles

2.2 THE RELATION BETWEEN MICRO AND MACRO VARIABLES

Plastic deformation on the asperity surfaces is defined by the terms in the asperity reference system(n, t) as shown in Fig.3. The (n, t) reference system evolves with asperity degradation as the plastic deformation occurs. The evolution includes rotation of the (n, t) system with respect to the fixed (N, T) reference system as shown in Fig.3. The macroscopic normal and shear stresses (σ_N, τ_T) for both aggregate-mortar and mortar-mortar interfaces, can be fully transformed into asperity stresses (σ_n, τ_t) as shown in Fig.3. The transformation must account the degradation of the asperity angles. For a given instant of loading, both macroscopic displacements and stresses can be transformed into asperity displacements and stresses as follows:

for mortar-mortar interface:

$$\begin{Bmatrix} \sigma_n \\ \tau_t \end{Bmatrix} = \begin{bmatrix} \cos^2 \alpha_m & 2 \sin \alpha_m \cos \alpha_m \\ -\sin \alpha_m \cos \alpha_m & \cos^2 \alpha_m - \sin^2 \alpha_m \end{bmatrix} \begin{Bmatrix} \sigma_N \\ \tau_T \end{Bmatrix}_{(m-m)} \dots \dots \dots (3)$$

$$\begin{Bmatrix} \delta_n \\ \delta_t \end{Bmatrix} = \begin{bmatrix} \cos \alpha_m & \sin \alpha_m \\ -\sin \alpha_m & \cos \alpha_m \end{bmatrix} \begin{Bmatrix} \delta_N \\ \delta_T \end{Bmatrix} \dots \dots \dots (4)$$

for aggregate-mortar interface:

$$\begin{Bmatrix} \delta_n \\ \delta_t \end{Bmatrix}_i = \begin{bmatrix} \sin \alpha_i & \cos \alpha_i \\ -\cos \alpha_i & \sin \alpha_i \end{bmatrix} \begin{Bmatrix} \delta_N \\ \delta_T \end{Bmatrix} \dots \dots \dots (5)$$

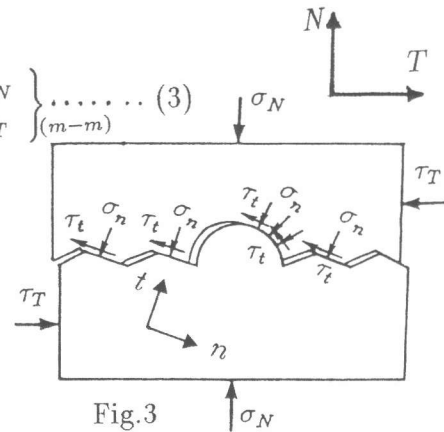


Fig.3 Macroscopic and Asperity Stresses

$$\begin{Bmatrix} \sigma_n \\ \tau_t \end{Bmatrix}_i = \begin{bmatrix} \sin^2 \alpha_i & 2 \sin \alpha_i \cos \alpha_i \\ -\sin \alpha_i \cos \alpha_i & \sin^2 \alpha_i - \cos^2 \alpha_i \end{bmatrix} \begin{Bmatrix} \sigma_N \\ \tau_T \end{Bmatrix}_{(a-m)} \quad (6)$$

where $\alpha_i = \alpha_n \sim \alpha_a$, $(m-m)$ and $(a-m)$ refer to both mortar-mortar and aggregate-mortar contacts.

2.3 MICROSCOPIC PLASTIC-FRACTURE FORMULATION

The present formulation follows the basic concepts of the theory of plasticity. These formulation will be carried out in the (n, t) reference system. The subsequent yield surface is assumed to change its size depending on the damage accumulated at each crack interface, i.e. the failure surface is a function of the damage parameter $\omega(W^p)$ as follows:

$$f = f(\sigma_i, \omega(W^p)) = 0 \quad (7)$$

where σ_i denotes the asperity stresses (σ_n, τ_t) and ω is the accumulated damage which is a function of the accumulated plastic work W^p after initial failure. The first postulate of the plasticity theory is the decomposition of the incremental displacement (δ_n, δ_t) into an elastic and plastic portions:

$$d\delta_j = d\delta_j^e + d\delta_j^p \quad (8)$$

where δ_j denotes the asperity displacements (δ_n, δ_t) . Another postulate is that only the elastic displacements induce stresses. Using Hook's law, this postulate can be expressed by

$$d\sigma_i = k_{ij}^e d\delta_j^e = k_{ij}^e (d\delta_j - d\delta_j^p) \quad (9)$$

where k_{ij}^e is the microscopic elastic stiffness tensor for the interface. The value of k_{ij}^e can be obtained from the corresponding macroscopic one through stress - displacement transformation matrices in eqs.3 ~ 6. Finally, in order to define the plastic displacement increments, a flow rule is used as follows:

$$d\delta_j^p = d\lambda \frac{\partial f}{\partial \sigma_j} \quad (10)$$

where $d\lambda$ is a non-negative scalar which can be determined from the consistency condition during loading. The consistency condition ($df=0$) can be expressed as:

$$df = \frac{\partial f}{\partial \sigma_i} d\sigma_i + \frac{\partial f}{\partial W^p} dW^p = 0 \quad (11)$$

where $dW^p = \sigma_i d\delta_i^p$. Finally, the elasto-plastic stiffness matrix for each interface can be written in the following form:

$$k_{ij}^{ep} = k_{ij}^e - \frac{k_{iq}^e \frac{\partial f}{\partial \sigma_p} \frac{\partial f}{\partial \sigma_q} k_{pj}^e}{\frac{\partial f}{\partial \sigma_m} k_{mn}^e \frac{\partial f}{\partial \sigma_n} + h}, \quad h = - \frac{\partial f}{\partial W^p} \sigma_i \frac{\partial f}{\partial \sigma_i} \quad (12)$$

Note that $\partial f / \partial W^p$ in eqs.11 and 12 will be a negative value for the hardening behavior and a positive value for the softening behavior.

2.4 MODIFIED MOHR - COULOMB FAILURE SURFACE

The subsequent yield surface is defined as a hyperbolic surface as follows:

$$f = \tau_t^2 - (C^* - \sigma_n \tan \phi^*)^2 + (C^* - \chi^* \tan \phi^*)^2 \quad (13)$$

The subsequent yield surface eq.13 is shown in Fig.4, and it may be recognized that the surface has Mohr-Coulomb surface as its asymptotic surface. The notations ϕ^* , C^* and χ^* are the mobilized friction angle, the cohesion, and the tensile strength(tension cutoff), which are not constant but depend on the plastic history through the damage parameter ω . All of these material parameters are used to consider the material nonlinearities. Referring to the previous work[6], the possible relations are suggested to be as follows:

$$C^* = C_0 \exp [-(m \omega)^2] \quad (14)$$

$$\begin{cases} \phi^* = \phi_0 + (\phi - \phi_0) \sqrt{2\omega - \omega^2} & \omega \leq 1 \\ \phi^* = \phi & \omega > 1 \end{cases} \quad (15)$$

$$\begin{cases} \chi^* = f_t (1 - \frac{\omega}{\omega_0}) & \omega \leq \omega_0 \\ \chi^* = 0 & \omega > \omega_0 \end{cases} \quad (16)$$

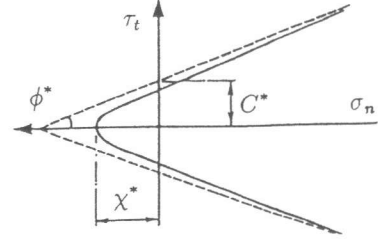


Fig.4 Hyperbolic Yield Surface

where m is a material parameter, C_0 , f_t , ϕ_0 and ϕ are the initial cohesion, the tensile strength, the initial friction angle and the final friction angle, respectively. All these relations are shown in Fig.5. From eq.13, the subsequent yield surface is expressed in terms of C^* , ϕ^* and χ^* parameters. Moreover, from eqs.14, 15 and 16, these parameters are assumed to be unique function of the damage parameter ω and defined to characterize the shape and size of the yield surface. Therefore, the function $\partial f / \partial W^p$ in eqs.11 and 12 can be elaborated as

$$\frac{\partial f}{\partial W^p} = \left(\frac{\partial f}{\partial C^*} \frac{\partial C^*}{\partial \omega} + \frac{\partial f}{\partial \phi^*} \frac{\partial \phi^*}{\partial \omega} + \frac{\partial f}{\partial \chi^*} \frac{\partial \chi^*}{\partial \omega} \right) \frac{\partial \omega}{\partial W^p} \quad (17)$$

The damage parameter is linked with the accumulated plastic work as follows:

$$\omega = \beta \int dW^p \quad (18)$$

where β is a material parameter.

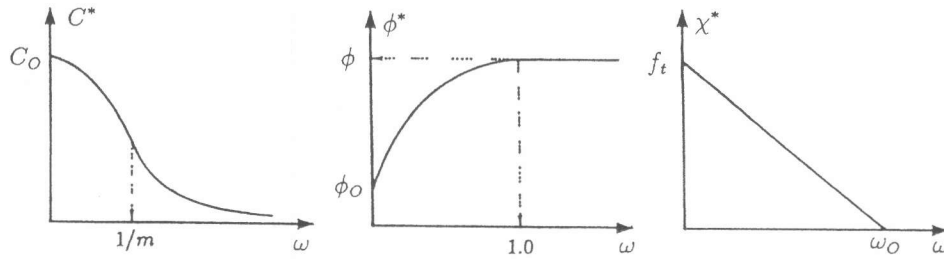


Fig.5 Possible Relations of $C^* - \omega$, $\phi^* - \omega$ and $\chi^* - \omega$

2.5 MACROSCOPIC STRESS - DISPLACEMENT RELATIONSHIP

Based on Voigt's model, the average stress increment for two kinds of contacts can be expressed as follows:

$$d\bar{\sigma}_{ij} = \frac{1}{S} \left(\int_{s_a} d\sigma_{ij}^{a-m} ds + \int_{s_m} d\sigma_{ij}^{m-m} ds \right) \quad (19)$$

Eq.19 yields the following equation:

$$d\bar{\sigma}_{ij} = \frac{S_a}{S} d\bar{\sigma}_{ij} (a - m) + \frac{S_m}{S} d\bar{\sigma}_{ij} (m - m) \quad (20)$$

Considering the case of homogenous strain state (i.e., $\bar{\epsilon}_{ij} = \bar{\epsilon}_{ij}(a-m) = \bar{\epsilon}_{ij}(m-m)$) with the help of eq.20, the incremental stress-displacement relation is given as follows:

$$d\bar{\sigma}_i = [\eta K_{ij}^{(ep) a-m} + (1 - \eta) K_{ij}^{(ep) m-m}] d\delta_j = K_{ij}^{(ep)} d\delta_j \quad (21)$$

where η is the percentage of the area of aggregate at interface with respect to the total surface area of crack. Both s_a and s_m denote the surface areas of aggregate-mortar and mortar-mortar interfaces. $K^{(ep)}$, $K^{(ep)a-m}$ and $K^{(ep)m-m}$ are the macroscopic elasto-plastic stiffness matrices for concrete and both interfaces. The notations $(m-m)$ and $(a-m)$ refer to both mortar-mortar and aggregate-mortar interfaces. In this study, the elastic macrostiffness of mortar-mortar interface is assumed to be as follows:

$$K_{ij}^e (\text{mortar} - \text{mortar interface}) = R K_{ij}^e (\text{concrete}) \quad (22)$$

The value of 'R' should be obtained experimentally. However, this value will be obtained to achieve a reasonable agreement with the test data. The elastic stress-displacement relation for concrete in eq.21 in a matrix form is given as follows:

$$\begin{Bmatrix} d\bar{\sigma}_N \\ d\bar{\sigma}_T \end{Bmatrix} = \begin{bmatrix} K_N & 0 \\ 0 & K_T \end{bmatrix} \begin{Bmatrix} d\delta_N \\ d\delta_T \end{Bmatrix}, \quad K_{ij}^e (\text{concrete}) = \begin{bmatrix} K_N & 0 \\ 0 & K_T \end{bmatrix} \quad (23)$$

where K_N and K_T are the initial normal and shear stiffnesses of the contact zone. Since the elastic behavior in any reference system is independent of plastic deformation on the asperity surfaces, the above relation can always be transformed into (n, t) system. Although the prediction of both K_N and K_T is necessary, however it is excluded in this paper. These values are measured from the experimental data.

3. VERIFICATION OF THE PROPOSED MODEL

In this section, a number of examples illustrating the constitutive law's performance are considered. In the beginning, the effect of the material parameter ' β ' in eq.19 both at mortar-mortar (β_a) and aggregate-mortar (β_m) interfaces on the behavior of concrete and on the degradation of the contact surfaces is shown in Fig.6. In Fig.6(a), the solid lines show the calculation results varying with the material parameter β_a with fixed material parameter $\beta_m = 0.9$. The results are compared with the experimental data of Millard, et al.[3]. The other solid lines in Fig.6(a) represent the degradation of the asperity angle at aggregate-mortar interface. Also, in Fig.6(b), the effects of material parameter β_m on the behavior and on the asperity angle at mortar-mortar contact are presented. In Fig.6(b), the value of the material parameter $\beta_a = 0.40$ is kept constant.

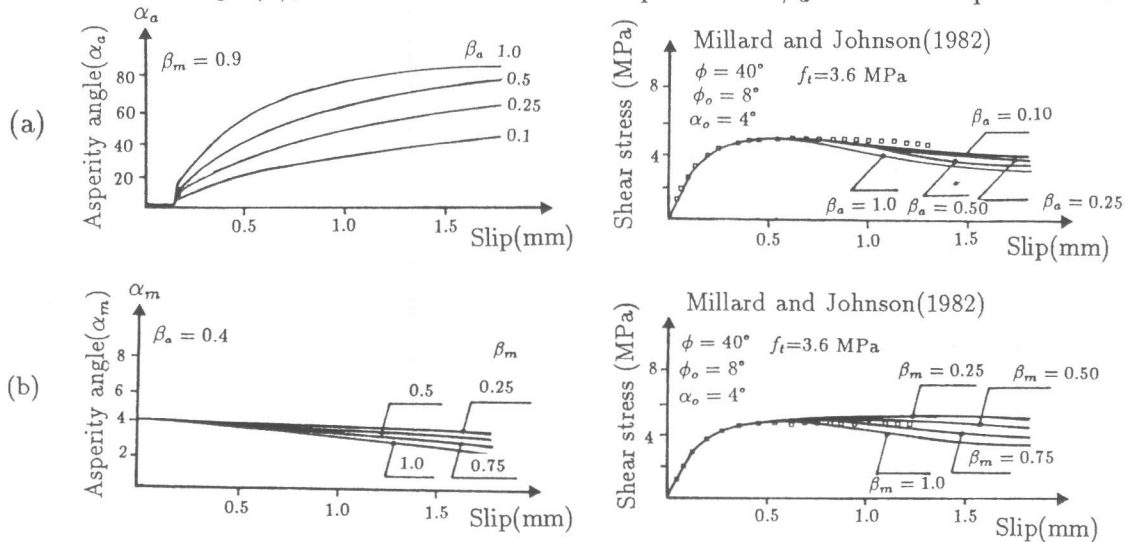


Fig.6 Effect of Material Parameter β

Fig.7 shows the prediction of the proposed model under variable concrete strength. The results are compared with the test data of Fenwick, et al.[1].

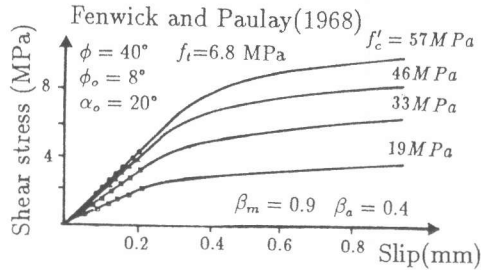


Fig. 7 Comparison with Test Data[1]

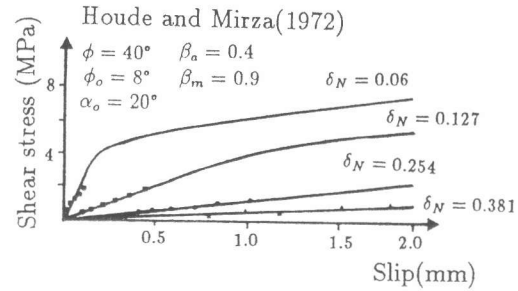


Fig. 8 Comparison with Test Data[2]

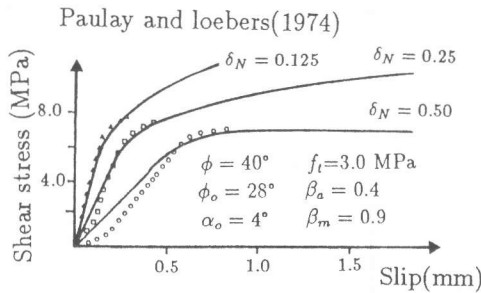


Fig. 9 Comparison with Test Data[4]

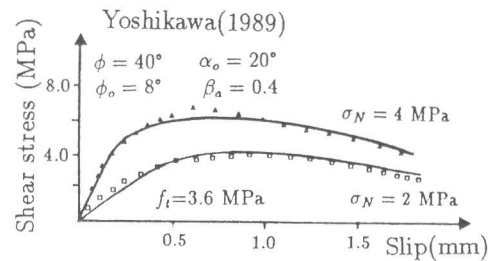


Fig. 10 Comparison with Ref.[5]

Figs.8 and 9 illustrates the comparison with the test data of Paulay, et al.[4] and Houde, et al.[2] for the cases of different constant crack widths. Fig.10 represents the numerical simulation for different constant applied stresses. The results are compared with Yoshikawa's model[5] for shear slip of cracked concrete.

4. CONCLUSIONS

A general constitutive law for shear stress transfer problem is proposed. A major feature of the proposed model is the development of an explicit relation between the increments of stresses and relative discontinuity displacements at all possible interfaces across the crack. Such a relation can be implemented in FEM computer codes and should render more realistic and reliable than those currently performed with more simple idealization. The numerical calculations showed that the proposed model can predict the shear transfer problem for concrete discontinuities. However, it is considered that the present model has its great advantage to deal with more general problems such as the effect of dilatancy, the cyclic behavior and the time effect. These phenomena are under investigation now.

REFERENCES

1. Fenwick, R. C. and Paulay, T., "Mechanisms of Shear Resistance of Concrete Beams," Journal of Struct. Div., ASCE, Vol.94, No.10, 1968, pp.2325-2350.
2. Houde, J. and Mirza, M. S., "Investigation of shear transfer across cracks by aggregate interlock," Res. Report No.72-06, Ecole Polytechnique de Montreal, , Canada, 1972.
3. Millard, S. G. and Johneson, R. D., "Shear Transfer in Cracked Reinforced Concrete," Magazine of Concrete Research, Vol.17, No.130, March, 1985, pp.3-15.
4. Paulay, T. and Loeber, P. J., "Shear Transfer by Aggregate Interlock," SP42, American Concrete Inst., 1974, pp.1-15.
5. Yoshikawa, H., Wu, Z. S. and Tanabe, T., "Analytical Model for Shear Slip of Cracked Concrete," Journal of Struct. Engrg., ASCE, Vol.15, No.4, April, 1989, pp.771-788.
6. Wu, Z. S. and Tanabe, T., "A Hardening-Softening Model of Concrete Subjected to Compressive Loading," Journal of Struct. Engrg., AIJ, Vol. 36B, 1990, pp.153-162.